# On monolithic and Chorin-Temam schemes for incompressible flows in moving domains

Reidmen Aróstica, Cristobal Bertoglio

# On monolithic and Chorin-Temam schemes for incompressible flows in moving domains

Reidmen Aróstica
Bernoulli Institute
University of Groningen
Groningen, 9747AG, The Netherlands

Cristóbal Bertoglio
Bernoulli Institute
University of Groningen
Groningen, 9747AG, The Netherlands

September 7, 2020

**Abstract**

Several time discretization schemes for the incompressible Navier-Stokes equations (iNSE) in moving domains have been proposed. Here we introduce them in a unified fashion, allowing a common well possedness and time stability analysis. It can be therefore shown that only a particular choice of the numerical scheme ensures such properties. The analysis is performed for monolithic and Chorin-Temam schemes. Results are supported by numerical experiments.

# 1 Introduction

Several works have been reported dealing with the numerical solution of the iNSE in moving domains within an Arbitrary Lagrangian Eulerian formulation (ALE), primarily in the context of fluid-solid coupling. In particular different choices of time discretization have been reported on [2,5,7–9,11–13,15,17]. To the best of the authors knowledge, only a few monolithic schemes have been thoroughly analyzed, e.g. in [4,12,15,17], while no analysis has been reported for Chorin-Temam (CT) methods. The goal of this work is therefore to assess well-posedness and unconditional energy balance of the iNSE-ALE for all reported monolithic and CT discretization schemes within a single formulation.

The reminder of this paper is structured as follows: Section 2 provides the continuous problem that will be studied. Section 3 introduces a general monolithic scheme that characterizes several approaches used in literature, well-posedness and energy stability are studied and discussed. Section 4 introduces the Chorin-Temam schemes where time stability is analyzed. Finally, Section 5 provides numerical examples testing our results.

# 2 The continuous problem

In the following, let us consider a domain $\Omega_0 \subset \mathbb{R}^d$ with $d = 2, 3$ and a deformation mapping $\mathcal{X} : \mathbb{R}^d \times \mathbb{R}_+ \mapsto \mathbb{R}^d$ that defines the time evolving domain $\Omega_t := \mathcal{X}(\Omega_0, t)$. We assume $\mathcal{X}$ a continuous mapping, 1-to-1 with continuous inverse. We denote $\mathbf{X} \in \mathbb{R}^d$ the cartesian coordinate system in $\Omega_0$ and $\mathbf{x}_t := \mathcal{X}(\mathbf{X}, t)$ the one in $\Omega_t$, by $F_t := \frac{\partial \mathbf{x}_t}{\partial \mathbf{X}}$ the deformation gradient, $F_t^{-1}$ its inverse and $J_t := det(F_t)$ its jacobian. Similarly, $Grad(\mathbf{g}) := \frac{\partial \mathbf{g}}{\partial \mathbf{X}}$, $Div(\mathbf{g}) := \frac{\partial}{\partial \mathbf{X}} \cdot \mathbf{g}$ denote the gradient and divergence operators, respectively, and $\epsilon^t(\mathbf{g}) := \frac{1}{2}(Grad(\mathbf{g})F_t^{-1} + F_t^{-T}Grad(\mathbf{g})^T)$ the symmetric gradient, for $\mathbf{g}$ a well-defined vector function. We consider the weak form of the iNSE in ALE form [14, Ch. 5]: Find $(\mathbf{u}(t), p(t)) \in \mathbf{H}_0^1(\Omega_0) \times L_0^2(\Omega_0)$ with $\mathbf{u}(0) = \mathbf{u}_{init}$ s.t.

$$\begin{aligned} \int_{\Omega_0} \rho J^t \partial_t \mathbf{u} \cdot \mathbf{v} + \rho J^t Grad(\mathbf{u}) F_t^{-1}(\mathbf{u} - \mathbf{w}) \cdot \mathbf{v} + J^t 2\mu\, \epsilon^t(\mathbf{u}) : \epsilon^t(\mathbf{v}) \\ - Div(J^t F_t^{-1}\mathbf{v})p + Div(J^t F_t^{-1}\mathbf{u})q = 0 \end{aligned} \tag{1}$$

for all $(\mathbf{v}, q) \in \mathbf{H}_0^1(\Omega_0) \times L_0^2(\Omega_0)$, $t > 0$, $\mathbf{u}_{init}, \mathbf{w}(t) \in \mathbf{H}_0^1(\Omega_0)$ given initial and domain velocities, where $\mathbf{H}_0^1(\Omega_0)$ is the standard Sobolev space of vector fields $\mathbf{u}$ defined on $\Omega_0$ with values in $\mathbb{R}^d$ s.t. $\mathbf{u} = \mathbf{0}$ on $\partial\Omega_0$, $L_0^2(\Omega_0)$ the standard square integrable space of functions $p$ s.t. $p(\mathbf{0}) = 0$. Notice that the flow at time $t$ is given by $\mathbf{u} \circ \mathcal{X}^{-1}(\cdot, t)$.

*Remark* 1. Although Dirichlet boundary conditions are used throughout this work, it can be extended straightforwardly to the Neumann case by including the so called *backflow stabilizations*, see e.g. [3]. Moreover, in the discrete case the extension of well-posedness results to the case with non-zero boundary conditions follow from trace theorem.

**Proposition 1.** *[6, Chap. 9] Provided* $(\mathbf{u}(t), p(t))$ *a solution of the formulation* (1)*, the following energy balance holds:*

$$\partial_t \int_{\Omega_0} \frac{\rho}{2} J^t |\mathbf{u}|^2 = - \int_{\Omega_0} J^t 2\mu |\epsilon^t(\mathbf{u})|^2 \tag{2}$$

*Remark* 2. Proposition 1 makes use of the *Geometric Conservation Law* (GCL) $\partial_t J^t = Div\left(J^t F_t^{-1}\mathbf{w}\right)$.

# 3 Monolithic schemes (first order in time)

Most of the numerical schemes for Problem (1) reported in the literature are first order and can be written as follows. Given a conforming finite element space $\mathbf{V} \times Q$ of $\mathbf{H}_0^1(\Omega_0) \times L_0^2(\Omega_0)$ for

velocity and pressure fields, the discrete problem of interest reads:
Find $(\mathbf{u}^{n+1}, p^{n+1}) \in \mathbf{V} \times Q$ s.t.

$$\mathcal{A}(\mathbf{u}^{n+1}, \mathbf{v}) - \mathcal{B}(\mathbf{v}, p^{n+1}) + \mathcal{B}(\mathbf{u}^{n+1}, q) = F(\mathbf{v}) \quad \forall (\mathbf{v}, q) \in \mathbf{V} \times Q \tag{3}$$

being

$$\begin{aligned}\mathcal{A}(\mathbf{u}, \mathbf{v}) := &\int_{\Omega_0} \rho \frac{J^{\star\star}}{\tau} \mathbf{u} \cdot \mathbf{v} + \int_{\Omega_0} \rho J^\star Grad(\mathbf{u}) F_\star^{-1} (\mathbf{u}^* - \mathbf{w}^{**}) \cdot \mathbf{v} + \int_{\Omega_0} J^\star 2\mu \epsilon^\star(\mathbf{u}) : \epsilon^\star(\mathbf{v}) \\ &+ \alpha \int_{\Omega_0} \frac{\rho}{2} \left( \frac{J^{n+1} - J^n}{\tau} - Div\left(J^\star F_\star^{-1} \mathbf{w}_h^{**}\right) \right) \mathbf{u} \cdot \mathbf{v} + \beta \int_{\Omega_0} \frac{\rho}{2} Div\left(J^\star F_\star^{-1} \mathbf{u}^*\right) \mathbf{u} \cdot \mathbf{v}\end{aligned} \tag{4}$$

with $\alpha, \beta \in \{0, 1\}$ given parameters, and

$$\mathcal{B}(\mathbf{u}, q) := \int_{\Omega_0} Div\left(J^\star F_\star^{-1} \mathbf{u}\right) q \quad \forall q \in Q, \quad \mathcal{F}(\mathbf{v}) := \int_{\Omega_0} \rho \frac{J^n}{\tau} \mathbf{u}^n \cdot \mathbf{v} \quad \forall \mathbf{v} \in \mathbf{V} \tag{5}$$

*Remark* 3. The term multiplying $\alpha$ is the discrete residual of GCL, while the one multiplying $\beta$ is a strongly consistent term vanishing for incompressible velocity fields.

Formulation (3) contains a wide family of reported methods:

- Using $\alpha = \beta = 0$: $(\star, \star\star, *, **) = (n, n, n+1, n)$ is used in [2], $(\star, \star\star, *, **) = (n, n, n, n)$ in [13] and $(\star, \star\star, *, **) = (n+1, n+1, n+1, n+1)$ in [10], and $(\star, \star\star, *, **) = (n, n+1, n, n+1)$ in [8].
- Using $\alpha = \beta = 1$: $(\star, \star\star, *, **) = (n, n+1, n, n+1)$ in [12], $(\star, \star\star, *, **) = (n, n+1, n, n)$ in [15] and $(\star, \star\star, *, **) = (n+1, n, n+1, n+1)$ in [17, 18].

*Remark* 4. Other methods such as second order approximations can be found in [11, 16] and Crank-Nicolson approaches in [5, 7].

**Proposition 2.** *By assuming well-posed, orientation-preserving deformation mappings, i.e.* $(J^n)_{n\in\mathbb{N}}$ *bounded in* $L^\infty(\Omega_0)$*,* $J^n > 0$ *for each* $n \geq 0$*, Problem* (3) *has unique solution for inf-sup stable finite element spaces if* $\left(2J^{\star\star} + J^{n+1} - J^n\right) > 0$ *and* $\alpha = \beta = 1$*.*

*Proof.* Since all operators are bounded, and inf-sup stable elements are used for velocity and pressure, it is enough to ensure that the bilinear form $\mathcal{A}$ is coercive. Indeed:

$$\begin{aligned}\mathcal{A}(\mathbf{u}, \mathbf{u}) = &\int_{\Omega_0} \frac{J^\star}{2\tau} \left( \frac{2J^{\star\star}}{J^\star} + \alpha \frac{J^{n+1} - J^n}{J^\star} \right) |\mathbf{u}|^2 + J^\star 2\mu |\epsilon^\star(\mathbf{u})|^2 \\ &+ \int_{\Omega_0} \frac{\rho}{2} Div\left(J^\star F_\star^{-1} \left((\beta - 1)\mathbf{u}^* - (\alpha - 1)\mathbf{w}^{**}\right)\right) |\mathbf{u}|^2\end{aligned} \tag{6}$$

being the last quantity strictly positive under the stated assumptions. □

**Corollary 3.** *Assuming* $\alpha = \beta = 1$*, Problem* (3) *is well posed when:*

- $3J^{n+1} - J^n > 0$ *if* $\star\star = n+1$*, i.e. a restriction on the time step size.*
- $J^{n+1} + J^n > 0$ *if* $\star\star = n$*, i.e. no restriction on the time step size.*

*No restrictions apply to* $\star, *, **$*.*

**Proposition 4.** *Under assumptions of Proposition 2 and* $\alpha = \beta = 1, \star\star = n$*, the scheme* (3) *is unconditionally stable.*

*Proof.* By setting $\mathbf{v} = \mathbf{u}^{n+1}$ in the bi-linear form (4), $q = p^{n+1}$ in forms (5) and manipulating terms as standard in literature, the energy equality follows:

$$\begin{aligned}\int_{\Omega_0} \rho \frac{J^{n+1}}{2\tau}|\mathbf{u}^{n+1}|^2 - \int_{\Omega_0} \rho \frac{J^n}{2\tau}|\mathbf{u}^n|^2 = &\int_{\Omega_0} \frac{\rho}{2\tau}(J^{n+1} - J^{\star\star})|\mathbf{u}^{n+1}|^2 + \int_{\Omega_0} \frac{\rho}{2\tau}(J^{\star\star} - J^n)|\mathbf{u}^n|^2 \\ &- \int_{\Omega_0} 2\mu J^\star |\epsilon^\star(\mathbf{u}^{n+1})|^2 - \int_{\Omega_0} \frac{\rho}{2\tau} J^{\star\star}|\mathbf{u}^{n+1} - \mathbf{u}^n|^2 \\ &+ \int_{\Omega_0} \frac{\rho}{2} Div(J^\star F_\star^{-1}(\mathbf{u}^* - \mathbf{w}^{**}))|\mathbf{u}^{n+1}|^2 \\ &- \int_{\Omega_0} \frac{\rho}{2}\alpha \frac{J^{n+1} - J^n}{\tau}|\mathbf{u}^{n+1}|^2 \\ &+ \int_{\Omega_0} \frac{\rho}{2} Div\left(J^\star F_\star^{-1}(\beta \mathbf{u}^* - \alpha \mathbf{w}^{**})\right)|\mathbf{u}^{n+1}|^2\end{aligned} \tag{7}$$

Thus, for $\alpha = \beta = 1$ and $\star\star = n$ the result follows. □

# 4 Chorin-Temam schemes

In the following, we describe a family of Chorin-Temam (CT) schemes for the iNSE-ALE problem, as we did for the monolithic case. Given $\widetilde{\mathbf{V}}$ a conforming space of $\mathbf{H}_0^1(\Omega_0)$ and $\widetilde{Q}$ a conforming space of $L_0^2(\Omega_0) \cap H^1(\Omega_0)$, $\tilde{\mathbf{u}}^0 \in \widetilde{\mathbf{V}}$, for $n \geq 0$:

1. **Pressure-Projection Step** $(\mathbf{PPS})_n$ Find $p^n \in \widetilde{Q}$ s.t.

$$\int_{\Omega_0} \frac{\tau}{\rho} J^\circ Grad(p^n) F_\circ^{-1} : Grad(q) F_\circ^{-1} = -\int_{\Omega_0} Div\left(J^\circ F_\circ^{-1}\tilde{\mathbf{u}}^n\right) q \quad \forall q \in \widetilde{Q} \tag{8}$$

2. **Fluid-Viscous Step** $(\mathbf{FVS})_{n+1}$ Find $\tilde{\mathbf{u}}^{n+1} \in \widetilde{\mathbf{V}}$ s.t.

$$\begin{aligned}\int_{\Omega_0} \rho J^{\star\star} \frac{\tilde{\mathbf{u}}^{n+1} - \tilde{\mathbf{u}}^n}{\tau} \cdot \mathbf{v} + \int_{\Omega_0} \rho J^\star Grad(\tilde{\mathbf{u}}^{n+1}) F_\star^{-1}(\tilde{\mathbf{u}}^n - \mathbf{w}^{**}) \cdot \mathbf{v} \\ + \int_{\Omega_0} J^\star 2\mu \epsilon^\star(\tilde{\mathbf{u}}^{n+1}) : \epsilon^\star(\mathbf{v}) - \int_{\Omega_0} Div(J^{\circ\circ} F_{\circ\circ}^{-1}\mathbf{v}) p^n \\ + \int_{\Omega_0} \frac{\rho}{2} \frac{J^{n+1} - J^n}{\tau} \tilde{\mathbf{u}}^{n+1} \cdot \mathbf{v} + \int_{\Omega_0} \frac{\rho}{2} Div\left(J^\star F_\star^{-1}(\tilde{\mathbf{u}}^n - \mathbf{w}^{**})\right) \tilde{\mathbf{u}}^{n+1} \cdot \mathbf{v} = 0 \quad \forall \mathbf{v} \in \widetilde{\mathbf{V}}\end{aligned} \tag{9}$$

The following energy estimate can be obtained under suitable conditions:

**Proposition 5.** *Under assumptions* $\circ = \circ\circ = \star\star = n$*, the solution to scheme* (8)-(9) *is unconditionally stable with*

$$\int_{\Omega_0} \rho \frac{J^{n+1}}{2\tau}|\tilde{\mathbf{u}}^{n+1}|^2 - \int_{\Omega_0} \rho \frac{J^n}{2\tau}|\tilde{\mathbf{u}}^n|^2 \leq -\int_{\Omega_0} J^\star 2\mu |\epsilon^\star(\tilde{\mathbf{u}}^{n+1})|^2 - \int_{\Omega_0} J^n \frac{\tau}{2\rho}|Grad(p^n) F_n^{-1}|^2. \tag{10}$$

*Proof.* As standard in literature, let us take $\mathbf{v} = \tilde{\mathbf{u}}^{n+1}$ in $(\mathrm{FVS})_{n+1}$, and $q = p^n$ in $(\mathrm{PPS})_n$. Adding both equalities and rewriting expressions, it follows:

$$\int_{\Omega_0} \rho \frac{J^{n+1}}{2\tau}|\tilde{\mathbf{u}}^{n+1}|^2 - \int_{\Omega_0} \rho \frac{J^n}{2\tau}|\tilde{\mathbf{u}}^n|^2 = \int_{\Omega_0} \frac{\rho}{2\tau}(J^{n+1} - J^{\star\star})|\tilde{\mathbf{u}}^{n+1}|^2 + \int_{\Omega_0} \frac{\rho}{2\tau}(J^{\star\star} - J^n)|\tilde{\mathbf{u}}^n|^2$$
$$- \int_{\Omega_0} \frac{\rho}{2\tau} J^{\star\star}|\tilde{\mathbf{u}}^{n+1} - \tilde{\mathbf{u}}^n|^2 - \int_{\Omega_0} J^\star 2\mu|\epsilon^\star(\tilde{\mathbf{u}}^{n+1})|^2$$
$$+ \int_{\Omega_0} Div\left(J^{\circ\circ} F_{\circ\circ}^{-1}(\tilde{\mathbf{u}}^{n+1} - \tilde{\mathbf{u}}^n)\right) p^n$$
$$+ \int_{\Omega_0} Div\left((J^{\circ\circ} F_{\circ\circ}^{-1} - J^\circ F_\circ^{-1})\tilde{\mathbf{u}}^n\right) p^n$$
$$- \int_{\Omega_0} \frac{\tau}{\rho} J^\circ |F_\circ^{-T} Grad(p^n)|^2 - \int_{\Omega_0} \frac{\rho}{2\tau}(J^{n+1} - J^n)|\tilde{\mathbf{u}}^{n+1}|^2 \tag{11}$$

Bounding the first divergence term using integration by parts and Cauchy-Schwartz inequality, it follows

$$\int_{\Omega_0} Div\left(J^{\circ\circ} F_{\circ\circ}^{-1}(\tilde{\mathbf{u}}^{n+1} - \tilde{\mathbf{u}}^n)\right) p^n \leq \int_{\Omega_0} \frac{\rho}{2\tau} J^{\circ\circ}|\tilde{\mathbf{u}}^{n+1} - \tilde{\mathbf{u}}^n|^2 + \int_{\Omega_0} \frac{\tau}{2\rho} J^{\circ\circ}|F_{\circ\circ}^{-T} Grad(p^n)|^2 \tag{12}$$

Thus, the following energy estimate can be obtained:

$$\int_{\Omega_0} \rho \frac{J^{n+1}}{2\tau}|\tilde{\mathbf{u}}^{n+1}|^2 - \int_{\Omega_0} \rho \frac{J^n}{2\tau}|\tilde{\mathbf{u}}^n|^2 \leq \int_{\Omega_0} \frac{\rho}{2\tau}(J^{n+1} - J^{\star\star})|\tilde{\mathbf{u}}^{n+1}|^2 + \int_{\Omega_0} \frac{\rho}{2\tau}(J^{\star\star} - J^n)|\tilde{\mathbf{u}}^n|^2$$
$$- \int_{\Omega_0} \frac{\rho}{2\tau} J^{\star\star}|\tilde{\mathbf{u}}^{n+1} - \tilde{\mathbf{u}}^n|^2 - \int_{\Omega_0} J^\star 2\mu|\epsilon^\star(\tilde{\mathbf{u}}^{n+1})|^2$$
$$+ \int_{\Omega_0} \frac{\rho}{2\tau} J^{\circ\circ}|\tilde{\mathbf{u}}^{n+1} - \tilde{\mathbf{u}}^n|^2 + \int_{\Omega_0} \frac{\tau}{2\rho} J^{\circ\circ}|F_{\circ\circ}^{-T} Grad(p^n)|^2$$
$$+ \int_{\Omega_0} Div\left((J^{\circ\circ} F_{\circ\circ}^{-1} - J^\circ F_\circ^{-1})\tilde{\mathbf{u}}^n\right) p^n$$
$$- \int_{\Omega_0} \frac{\tau}{\rho} J^\circ |F_\circ^{-T} Grad(p^n)|^2 - \int_{\Omega_0} \frac{\rho}{2\tau}(J^{n+1} - J^n)|\tilde{\mathbf{u}}^{n+1}|^2 \tag{13}$$

From estimate (13) it follows that whenever $\circ = \circ\circ = \star\star = n$ unconditional energy stability is attained, where $\star$ remains free of choice. □

# 5 Numerical examples

We consider a rectangular domain with opposite vertices $\{(0,-1),(6,1)\}$ where the iNSE-ALE formulation (1) will be simulated over the interval $[0,2]\,[s]$ with non-zero initial condition of the form $\mathbf{u}(0) := \gamma(1-\mathbf{X}_1^2)\mathbf{X}_0(6-\mathbf{X}_0)$, $\gamma = 0.001$. The domain is deformed using $\mathcal{X}(\mathbf{X},t) := \big((1+0.9sin(8\pi t))\mathbf{X}_0,\, \mathbf{X}_1\big)$.

Discretization setup for Formulation (3) and (8)-(9) is done choosing a time step $\tau = 0.01$ and space triangulation with elements diameter $h \approx 0.01$, implemented through FEniCS [1] using Python for interface and postprocessing.

To exemplify the theoretical results from previous sections, four schemes are taken into account. Monolitic (M) Formulation (3) is taken with linearized convective term and implicit treatment, i.e., $(\star, *, **) = (n+1, n, n+1)$ where for $\star\star$ we consider two choices, denoted M $\star\star = n$ and M $\star\star = n+1$. For both cases the space discretization is carried out with $\mathbf{V}/Q = [\mathbb{P}_2]^d/\mathbb{P}_1$ Lagrange finite elements. Similarly, Chorin-Temam (CT) scheme (9)-(8) is taken with linearized convective term and implicit treatment, i.e. $(\star, **, \circ, \circ\circ) = (n+1, n+1, n, n)$ with

$\star\star$ as before, denoting each scheme by CT $\star\star = n$ and CT $\star\star = n+1$ with space discretization done through $\widetilde{\mathbf{V}}/\widetilde{Q} = [\mathbb{P}_1]^d/\mathbb{P}_1$ elements. In all cases $\alpha = \beta = 1$.

The results are assessed using time-dependent normalized parameters $\hat{\delta}_{\mathrm{M}} := \delta_{\mathrm{M}}/E^{\star}_{st}, \hat{\delta}_{\mathrm{CT}} := \delta_{\mathrm{CT}}/E^{\star}_{st}$ defined as:

$$\delta_M^{n+1} := D^{n+1} + E^{\star}_{st} + \int_{\Omega_0} \frac{\rho J^{\star\star}}{2\tau} |\mathbf{u}^{n+1} - \mathbf{u}^n|^2, \quad \delta_{CT}^{n+1} := D^{n+1} + E^{\star}_{st} + \int_{\Omega_0} \frac{\tau J^{\circ}}{2\rho} |F_{\circ}^{-T} Grad(p^n)|^2$$
$$D^{n+1} := \int_{\Omega_0} \frac{\rho}{2\tau} \left( J^{n+1} |\mathbf{u}^{n+1}|^2 - J^n |\mathbf{u}^n|^2 \right), \quad E^{\star}_{st} = \int_{\Omega_0} 2\mu J^{\star} |\epsilon^{\star}(\mathbf{u}^{n+1})|^2 \tag{14}$$

Figure 1 shows $\hat{\delta}_{\mathrm{M}}, \hat{\delta}_{\mathrm{CT}}$ values for each tested scheme. Propositions 4 and 5 are confirmed since $\hat{\delta}_{\mathrm{M}} = 0$ and $\hat{\delta}_{\mathrm{CT}} \leq 0$ if $\star\star = n$. For $\star\star = n+1$, peaks appearing throughout the simulation are defined by the sign change of domain velocity, i.e. in the change from expansion to contraction. Importantly, the spurious numerical energy rate related to discretization of the GCL condition appear to be positive in expansion, therefore being a potential source of numerical instabilities.

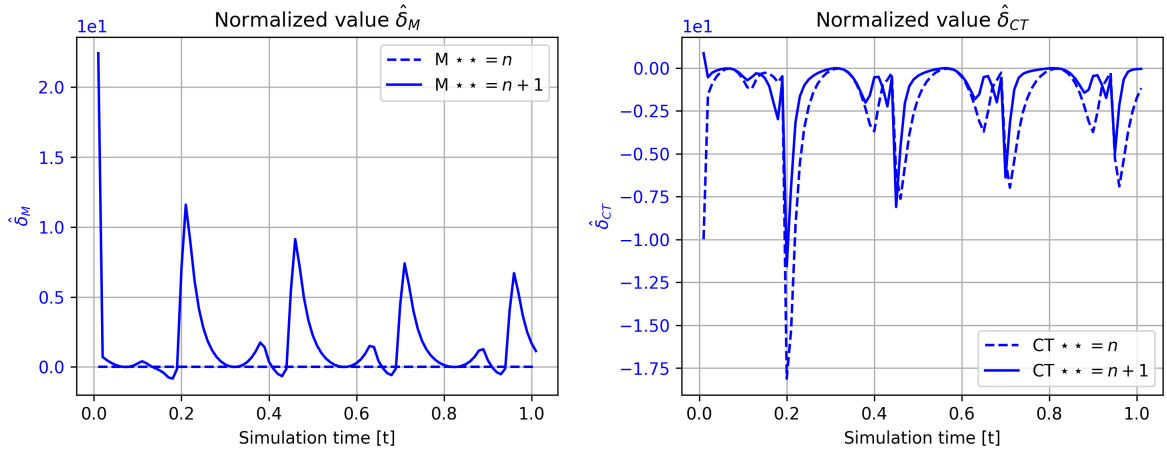


Figure 1: Summary of the numerical experiment in terms of energy balance. Left: Monolithic residual error values $\hat{\delta}_{\mathrm{M}}$; Right: Chorin-Temam residual error values $\hat{\delta}_{\mathrm{CT}}$.

## 6 Conclusion

Reported first order time discretization schemes for the iNSE-ALE have been reviewed, theoretically analyzed and numerically assessed. For the monolithic case, two schemes lead to well-posed energy-stable problems whenever $\alpha = \beta = 1$ with $\star\star = n$ as studied by [12, 15, 17, 18]. To the best of the authors knowledge, the unconditionally stable Chorin-Temam scheme derived in this work has not been reported yet.

## References


[1] M. Alnæs, J. Blechta, J. Hake, A. Johansson, B. Kehlet, A. Logg, C. Richardson, J. Ring, M. E. Rognes, and G. N. Wells. The fenics project version 1.5. *¡p¿Archive of Numerical Software*, Vol 3:¡strong¿Starting Point and Frequency: ¡/strong¿Year: 2013¡/p¿–, 2015.

[2] S. Basting, A. Quaini, S. Čanić, and R. Glowinski. Extended ALE method for fluid–structure interaction problems with large structural displacements. *Journal of Computational Physics*, 331:312–336, Feb. 2017.

[3] C. Bertoglio, A. Caiazzo, Y. Bazilevs, M. Braack, M. Esmaily, V. Gravemeier, A. L. Marsden, O. Pironneau, I. E. Vignon-Clementel, and W. A. Wall. Benchmark problems for numerical treatment of backflow at open boundaries. *International journal for numerical methods in biomedical engineering*, 34(2):e2918, 2018.

[4] B. Burtschell, D. Chapelle, and P. Moireau. Effective and energy-preserving time discretization for a general nonlinear poromechanical formulation. *Computers & Structures*, 182:313–324, Apr. 2017.

[5] L. Failer, P. Minakowski, and T. Richter. On the impact of fluid structure interaction in blood flow simulations: Stenotic coronary artery benchmark, 2020.

[6] L. Formaggia, A. Quarteroni, and A. Veneziani, editors. *Cardiovascular Mathematics*. Springer Milan, 2009.

[7] A. Hessenthaler, O. Röhrle, and D. Nordsletten. Validation of a non-conforming monolithic fluid-structure interaction method using phase-contrast MRI. *International Journal for Numerical Methods in Biomedical Engineering*, 33(8):e2845, Feb. 2017.

[8] M. Landajuela, M. Vidrascu, D. Chapelle, and M. A. Fernández. Coupling schemes for the FSI forward prediction challenge: Comparative study and validation. *International Journal for Numerical Methods in Biomedical Engineering*, 33(4):e2813, July 2016.

[9] U. Langer and H. Yang. Numerical simulation of fluid-structure interaction problems with hyperelastic models: A monolithic approach, 2014.

[10] U. Langer and H. Yang. Robust and efficient monolithic fluid-structure-interaction solvers. *International Journal for Numerical Methods in Engineering*, 108(4):303–325, Feb. 2016.

[11] J. Liu and A. L. Marsden. A unified continuum and variational multiscale formulation for fluids, solids, and fluid–structure interaction. *Computer Methods in Applied Mechanics and Engineering*, 337:549–597, Aug. 2018.

[12] A. Lozovskiy, M. A. Olshanskii, and Y. V. Vassilevski. A quasi-lagrangian finite element method for the navier–stokes equations in a time-dependent domain. *Computer Methods in Applied Mechanics and Engineering*, 333:55–73, May 2018.

[13] C. M. Murea and S. Sy. Updated lagrangian/arbitrary lagrangian-eulerian framework for interaction between a compressible neo-hookean structure and an incompressible fluid. *International Journal for Numerical Methods in Engineering*, 109(8):1067–1084, June 2016.

[14] T. Richter. *Fluid-structure Interactions*. Springer International Publishing, 2017.

[15] S. Smaldone. *Numerical analysis and simulations of coupled problems for the cariovascular system*. Theses, L'UNIVERSITÉ PIERRE ET MARIE CURIE - Paris VI , Oct. 2014.

[16] L. Tallec and P. Hauret. Energy conservation in fluid-structure interactions. 01 2003.

[17] P. L. Tallec and J. Mouro. Fluid structure interaction with large structural displacements. *Computer Methods in Applied Mechanics and Engineering*, 190(24-25):3039–3067, Mar. 2001.

[18] Y. Wang, P. K. Jimack, M. A. Walkley, and O. Pironneau. An energy stable one-field monolithic arbitrary lagrangian-eulerian formulation for fluid-structure interaction, 2020.